

Pavement Distress Analysis based on Dual-Tree Complex Wavelet Transform

Jinjiang Wang¹ and Robert X. Gao¹⁺

Abstract: Pavement distress identification and classification are critically important for pavement health management. This paper presents a new method for pavement distress identification based on the dual-tree complex wavelet transform (DT-CWT). It takes a multi-scale and multi-resolution approach to decomposing a pavement image into multi-level subbands, with high frequency subbands containing distress features selected as the subbands of interest. After thresholding is performed on wavelet coefficients to reduce noise, multi-level sub-images were constructed through inverse DT-CWT. The merit of the presented method rests on the shift invariance and good directional selectivity in DT-CWT while maintaining high computational efficiency. Numerical and experimental analysis results confirmed its substantial performance enhancement over ordinary Discrete Wavelet Transform (DWT), as commonly reported in literature.

Key words: DWT; DT-CWT; Pavement distress.

Introduction

Pavement deteriorates over time due to traffic loading and environmental factors [1]. The most commonly seen pavement distress is surface cracking, which can be classified as longitudinal, transverse, diagonal, block, and alligator. Traditionally, pavement distress evaluation is conducted manually by engineers who visually inspect the distressed surfaces. Such evaluation involves high degrees of subjectivity, is labor intensive, and is sometimes not productive. With the advancement of automated video imaging techniques, pavement distress measurement for pavement management has gained new interest [2, 3]. In principle, automated techniques use video cameras installed in a moving vehicle to capture images of pavement. The images are subsequently processed to recognize and quantify the degree of pavement distress.

Effective pavement image processing is an active research area, and many efforts have been reported on developing pavement distress detection and recognition algorithms. Specifically, thresholding and edge detection are widely used for extracting features on pavement distress from recorded images. Traditional edge detection techniques, such as gradient based edge detector, Laplacian of Gaussian, zero crossing, and Canny edge detector, perform analysis at only one spatial scale. As a result, they are sensitive to background noise [4]. Since pavement images have various details at different scales, wavelet transform has been widely investigated for edge detection in pavement images, given its capability in multi-scale singularity detection, which corresponds to distress in pavement images [5]. Zhou *et al* proposed a pavement distress detection algorithm based on discrete wavelet transform

(DWT), by which the image is decomposed into different frequency subbands [6-7]. The magnitudes of wavelet coefficients represent the level of distress. In Javidi *et al* two base wavelets, defined as partial derivatives of a two-dimensional smoothing cubic spline wavelet function, are applied to measuring the wavelet coefficient maxima across the scales [8]. The crack pixels in pavement distress image are separated from the background noise.

The multi-scale nature of wavelet transform and its general robustness to noise makes it an attractive tool for pavement image processing. Many wavelet-based pavement distress identification methods reported in the literature involved the decimated discrete wavelet transform, which is computationally efficient [9]. A common drawback, however, is that such methods also suffer from shift variance and lack of directionality. Both features, however, are required for multi-scale analysis. The undecimated versions of wavelet transform, such as ridgelet transform and beamlet transform, are free from shift variance. Accordingly, they have been investigated for pavement distress analysis [10-11]. Similarly, an undecimated wavelet transform integrated with a trous algorithm is investigated in Wang *et al* for multi-scale edge detection [12]. The result shows that it outperforms the conventional edge detection techniques. However, undecimated wavelet decomposition requires higher computational load and yields high redundancy in the computed wavelet coefficients, making the subsequent computational processing (e.g., edge detection and classification) expensive [9].

To tackle the above problems, a new approach to pavement distress analysis based on the dual-tree complex wavelet transform (DT-CWT) [9] is investigated in this paper. DT-CWT is characterized by shift invariance and directional selectivity as required for pavement distress identification, and maintains high computation efficiency. Multi-scale and multi-resolution analysis using DT-CWT is performed on pavement images to obtain multi-level subband information, and wavelet thresholding technique is applied to reducing noise at each level. The selected subband information is then used to construct the sub-image for distress analysis. Numerical and experimental results demonstrate

¹ Department of Mechanical Engineering, University of Connecticut, Storrs, CT, USA.

⁺ Corresponding Author: E-mail rgao@engr.uconn.edu

Note: Paper presented at the International Workshop on Smart and Resilient Transportation held April 16-17, 2012 at Virginia Tech, USA; Revised August 3, 2012; Accepted August 4, 2012.

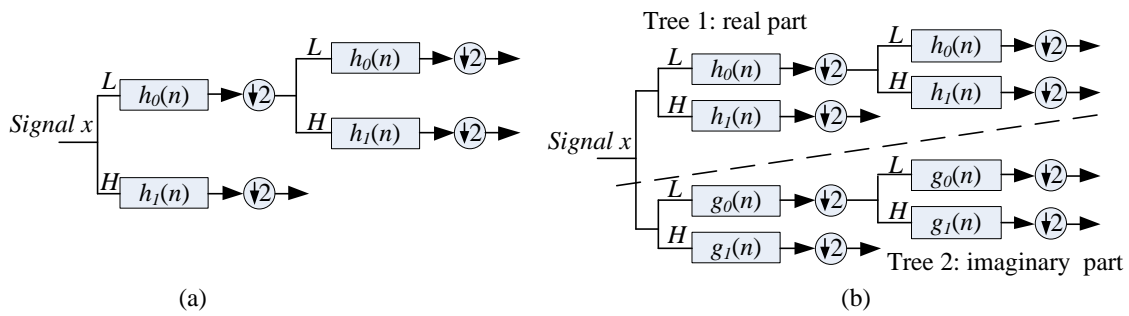


Fig. 1. Illustration of Wavelet Decompositions of a) DWT and b) DT-CWT.

that DT-CWT presents a substantial performance enhancement in distress detection over ordinary Discrete Wavelet Transform (DWT).

The rest of the paper is structured as follows. After introducing the theoretical background of dual-tree complex wavelet transform, details of its application to pavement distress analysis are discussed. Performance comparison with DWT is also provided. The effectiveness of the technique is experimentally evaluated. Finally, conclusions are then drawn.

Theoretical Background

Wavelet transform is a signal decomposition technique, which, by stretching and shifting a base wavelet along the timeline, quantifies the degree of matching or correlation between the base wavelet (which is mathematically defined) and the signal. Compared to the Fourier transform that involves infinitely oscillating sinusoidal basis functions, wavelet transform is based on locally oscillating functions, making it well suited for multi-resolution time-frequency analysis. Using the base wavelets $\psi(t)$ and scaling function $\phi(t)$, a one-dimensional real-valued signal $x(t)$ can be decomposed as:

$$x(t) = \sum_{n=-\infty}^{n=\infty} c(n)\phi(t-n) + \sum_{j=0}^{\infty} \sum_{n=-\infty}^{\infty} d(j,n)2^{j/2}\psi(2^j t-n) \tag{1}$$

where $c(t)$ represents a set of scaling coefficients, and $d(j, n)$ denotes the wavelet coefficients. By applying low-pass filtering $h_0(n)$, high-pass filtering $h_1(n)$, upsampling, and downsampling operations, the above wavelet decomposition can be implemented in a computationally efficient fashion as discrete wavelet transform (DWT). A typical decimated decomposition process of DWT is shown in Fig. 1a.

Although DWT in the decimated form has been widely used in image compression and restoration, it suffers from two main limitations: 1) lack of shift invariance and 2) low directional selectivity. As a result, a small shift in the input image may lead to a very different set of wavelet coefficients in the output. Because of the low directional selectivity resulting from the wavelet filters being separable and real, it is difficult to accurately recognize diagonal features, which is important in pavement distress analysis.

Complex wavelet transform can solve these two problems by emphasizing positive frequency and rejecting negative frequency that occur in real DWT [9]. However, it is difficult to implement inverse transform in complex wavelet transform, which is needed

for image compression and restoration. In comparison, the dual-tree complex wavelet transform [9] aims to enable perfect reconstruction using complex wavelet, by means of two parallel decimated filter band trees, with real-valued coefficients generated in each tree. It exhibits the properties of complex wavelet transform in shift invariance and good directionality. To analyze a one-dimensional real-valued signal, DT-CWT decomposition can be expressed by a complex shifted and dilated mother wavelet $\psi(t)$ and scaling function $\phi(t)$ as:

$$x(t) = \sum_{i \in Z} s_{j_0,l} \phi_{j_0,l}(t) + \sum_{j \geq j_0, l \in Z} c_{j,l} \psi_{j,l}(t) \tag{2}$$

$$\phi_{j_0,l}(x) = \phi_{j_0,l}^r(x) + \sqrt{-1} \phi_{j_0,l}^i(x)$$

$$\psi_{j,l}(x) = \psi_{j,l}^r(x) + \sqrt{-1} \psi_{j,l}^i(x)$$

where $s_{j_0,l}$ is a set of scaling coefficient, $c_{j,l}$ is a set of complex wavelet coefficients, and j and l refer to the index of shifts and dilations where Z is a natural number. The superscripts r and i denote the real and imaginary part, respectively, which are computed using separate filter banks such as low-pass/high-pass filter pair $h_0(n)$ and $h_1(n)$ for the real part, and low-pass/high-pass filter pair $g_0(n)$ and $g_1(n)$ for the imaginary part, as illustrated in Fig. 1b.

For image processing, the DWT process applies one separable low-pass/high-pass filter pair on the row and column elements of an image, and thus produces four sub-images (LL, LH, HL, HH) at each level, as shown in Fig. 2a. The sub-image LL is the approximation of the original image, whereas the sub-images LH and HL keep the main information in the horizontal and vertical directions, respectively. Sub-image HH contains the diagonal features. This means that DWT has only three-directional (0° , 45° , 90°) selectivity. For DT-CWT, it applies two low-pass/high-pass pairs on the row and column of the image, thus generating one approximate image LL, and six sub-images (two LH, two HL, and two HH) of complex coefficients at each level [13]. These six sub-images are oriented at the angles of $\pm 15^\circ$, $\pm 45^\circ$, and $\pm 75^\circ$, as illustrated in Fig. 2b. Therefore, DT-CWT enables better resolution and directionality selectivity as compared to DWT. This is essential in pavement distress analysis.

DT-CWT for Pavement Distress Analysis

A pavement distress image is mainly composed of three types of information: 1) non-uniform background (low-frequency signal), 2)

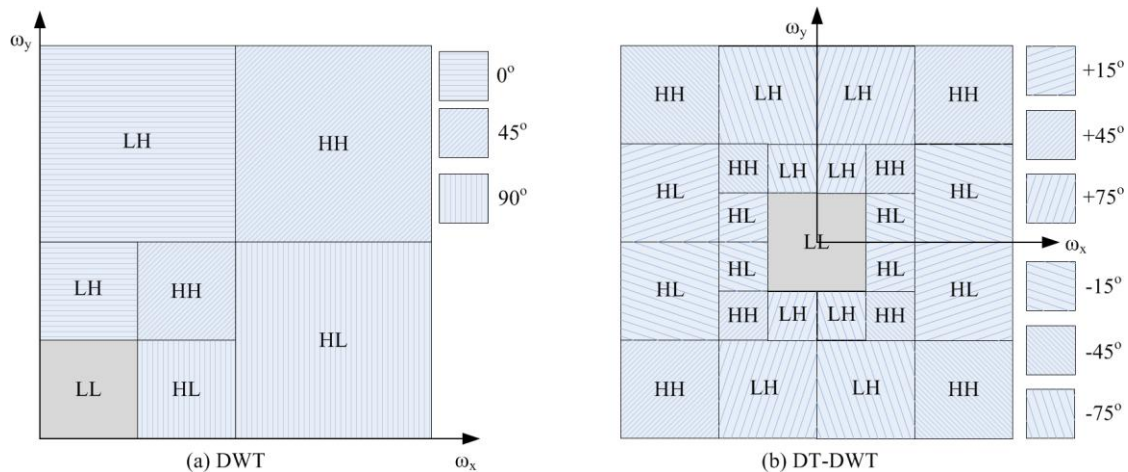


Fig. 2. Bandwidth and Orientation of Sub-images Resulting from a) DWT and b) DT-CWT Two-Level Decomposition.

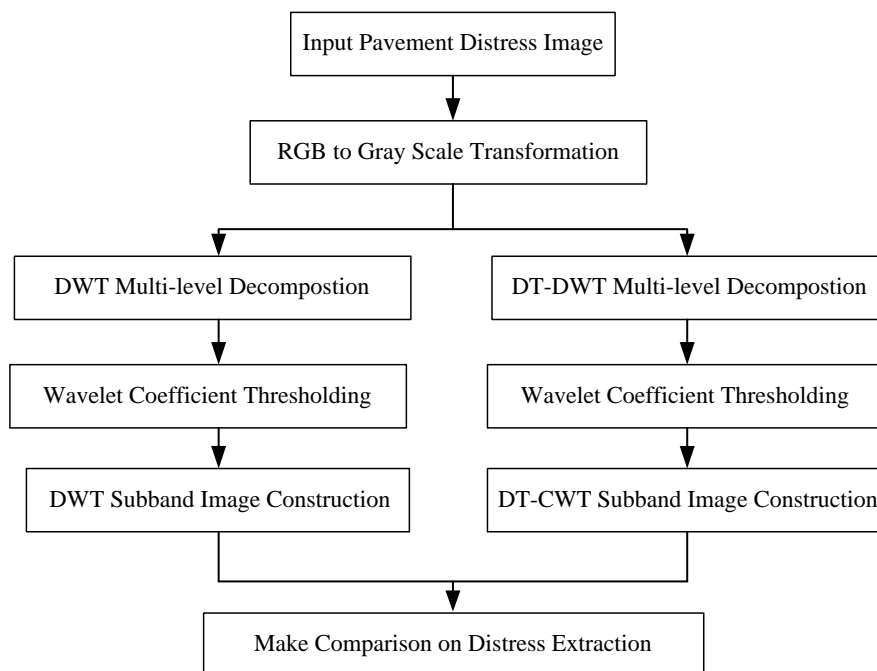


Fig. 3. Pavement Distress Analysis Based on DWT and DT-CWT.

pavement distress (e.g., crack, high frequency at the distress edge), and 3) noise from heterogeneous materials and granularity (high frequency, but low amplitude random signal) [3]. Through multi-resolution and multi-scale analysis enabled by the wavelet transform, these three types of information can be decomposed into different frequency subbands. Generally, the background information resides in the low frequency subband (LL) as an approximated or smoothed original distress image. The distress and noise caused by heterogeneous material are transformed into the high frequency subbands (HL, LH, HH) with different amplitudes for different wavelet coefficients. By using wavelet thresholding methods, the high-amplitude wavelet coefficients representing pavement distress can be extracted. Based on this consideration, a multi-scale pavement distress analysis method using dual-tree complex wavelet transform (DT-CWT) is developed, as shown in Fig. 3. To illustrate its merit in shift invariance and directional selectivity as required in pavement distress analysis, the ordinary

DWT is performed as well for comparison.

A pavement image is first decomposed into multi-level frequency subbands by DWT and DT-CWT, respectively. Specifically at each level, the image is decomposed into one low frequency subband LL and three high frequency subbands, labeled as HL, LH, and HH. The high frequency subbands preserve the distress information in the horizontal, vertical, and diagonal directions. The DT-CWT decomposes the pavement image into one low frequency subband and six high frequency subbands, which preserve the distress information in the direction of $\pm 15^\circ$, $\pm 45^\circ$, and $\pm 75^\circ$, respectively. To extract the distress information in the pavement image, the wavelet coefficients in the high frequency subbands (HL, LH, HH) are chosen to construct the distress image by removing the background.

Since noise from a heterogeneous material also resides in the high frequency subbands and is represented as low-amplitude wavelet coefficient, thresholding is then performed to suppress the noise.

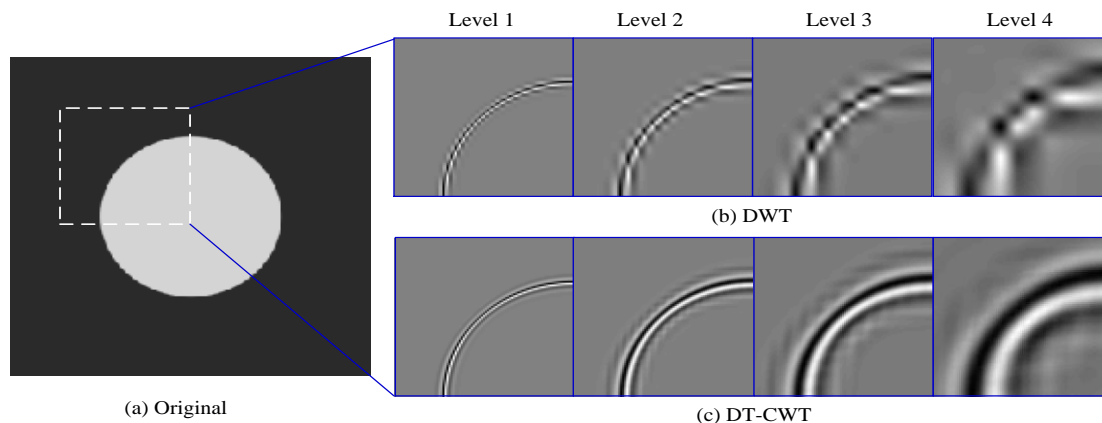


Fig. 4. Circular Disc Image [12] with Obtained Multi-level Edge Sub-images Using b) DWT and c) DT-CWT.

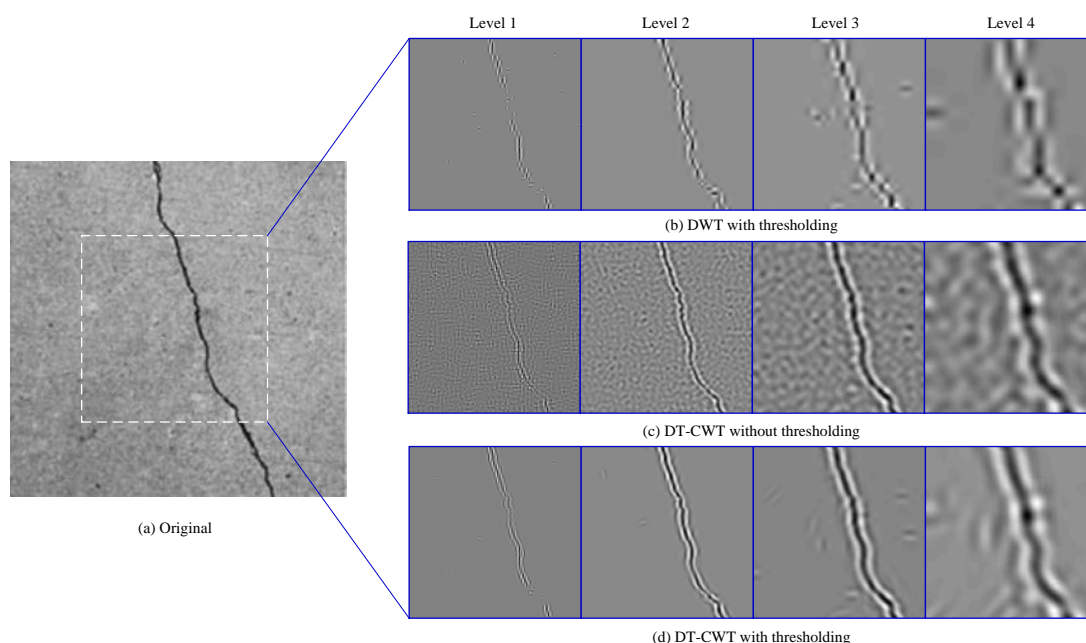


Fig. 5. a) Pavement Distress Image and Multi-level Subband Decomposition Using b) DWT with Thresholding, c) DT-CWT Without Thresholding and d) DT-CWT with Thresholding.

There are typically two thresholding methods, namely soft-thresholding (also called shrinkage function) and hard-thresholding [14]. Soft-thresholding takes the argument and shrinks it toward zero by the threshold T as:

$$\eta_T(x) = \text{sgn}(x) \bullet \max(|x| - T, 0) \tag{3}$$

Hard-thresholding keeps the argument if it is larger than the threshold T , expressed as:

$$\psi_T(x) = x \bullet I\{|x| > T\} \tag{4}$$

Otherwise, the argument is set to be zero. The value of the threshold is determined according to the VisaShrink method [15] as:

$$T = \sigma \sqrt{2 \log M} \tag{5}$$

where σ denotes the noise variance, and M is the number of samples. In the present study, hard-thresholding is chosen for its simplicity

and complex-valued property of wavelet coefficients in DT-CWT. After performing thresholding, the high-amplitude wavelet coefficients representing the distress are preserved in the high frequency subbands, and are used to construct distress image based on the inverse wavelet transform.

At each level/scale of wavelet transform, DT-CWT has six subbands that preserve the information with different orientations. This gives it better directional selectivity in the constructed distress image as compared to the DWT. To show its merit, an image of circular disc [12], with its edge simulating the crack in pavement image at different orientations, is used as an input. The high-frequency subbands (HL, LH, HH) of DWT and CWT are used to construct the edge sub-images at four different levels, as shown in Fig. 4. The results show that near-perfect edge information of circular disc has been extracted by DT-CWT at different levels, confirming its merit in shift invariance and good directional selectivity. In contrast, the sub-images obtained by DWT are associated with ringing effect and low resolution.

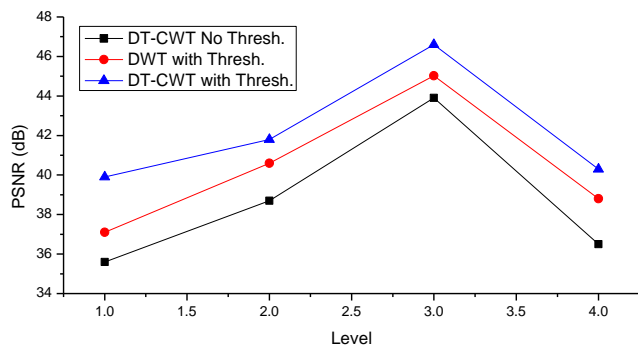


Fig. 6. PSNR Analysis Result for Multi-level Sub-images.

Experimental Evaluation

The performance of the developed image processing method is evaluated using different pavement images for different distress types and severities, and the results of DT-CWT and DWT for one distress image with diagonal crack are presented in Fig. 5.

For purpose of comparison, the results of constructing multi-scale, sub-images of the crack using DWT with thresholding, DT-CWT without thresholding, and DT-CWT with thresholding are illustrated in Fig. 5b-d, respectively. The effect of ringing and discontinuity can be seen in Fig. 5b, associated with DWT. The result from DT-CWT is significantly better. Especially when wavelet thresholding is applied, the noise present in the sub-images of Fig. 5c is further removed, as shown in Fig. 5d, indicating the effect of thresholding for distress edge retention.

To quantitatively evaluate the performance of DT-CWT and DWT, the experimental results presented above are analyzed using the criterion of peak-signal-to-noise-ratio (PSNR). The criterion measures the similarity between the extracted distress feature and the original image as the ground truth image in image segmentation [13] and compression [16]. It is based on the variance of difference between the obtained sub-image and original image, expressed as:

$$r(x, y) = I(x, y) - \hat{I}(x, y) \quad (6)$$

where $I(x, y)$ and $\hat{I}(x, y)$ are the normalized pixel values in obtained sub-image and original image, respectively. The variance is calculated as:

$$\sigma_r^2 = \frac{1}{M \cdot N} \sum_{x=1}^M \sum_{y=1}^N r^2(x, y) \quad (7)$$

where M and N are the pixel numbers in the row and column of the image, respectively. As a result, PSNR is defined based on the variance of the difference as:

$$PSNR(dB) = 10 \log_{10} \left(I / \sigma_r^2 \right) \quad (8)$$

A high value of $PSNR$ indicates a high similarity between the obtained sub-image and the original image. In Fig. 6, the calculated $PSNR$ values of multi-level sub-images of DT-CWT without thresholding, DWT with thresholding, and DT-CWT with thresholding are illustrated. It is seen that the $PSNR$ values of

multi-level sub-images using DT-CWT with thresholding are better than the ones using the other two methods. Due to noise deterioration, the $PSNR$ values of sub-images using DT-CWT without thresholding are less than that from DWT with thresholding. Of these three methods, the sub-images at level 3 present the highest $PSNR$ value.

Conclusion

Advanced image processing technique is critical to automated distress evaluation and classification for pavement distress identification and maintenance. A DT-CWT-based multi-scale distress analysis method for distress feature extraction is presented in this study. Compared to the ordinary DWT reported in the literature, the DT-CWT approach has yielded better performance due to its inherent shift invariance and high directional selectivity. The method is evaluated numerically and experimentally, and good results have been obtained. The multi-scale analysis capability of the developed method provides higher flexibility and insight into pavement distress evaluation. The DT-CWT algorithm has been implemented using two separable DWTs, thus maintaining high computational efficiency for real-time applications. Research is being continued to analyze the effect of scale and features selection for pavement evaluation and classification.

Acknowledgment

The authors would like to express their appreciation for Shaopeng Liu for his help in obtaining pavement images.

Reference

1. Said, S.F., Hakim H., Carlsson H., and Wiman L.G. (2011). Fatigue Life Evaluation of Flexible Pavement, *International Journal of Pavement Research and Technology*, 4(2), pp. 80-88.
2. Wang, L.B. and Lai, J.S. (2009). Quantification of Specific Surface Area of Aggregates Using an Imaging Technique, *International Journal of Pavement Research and Technology*, 2(1), pp. 13-19.
3. Cheng, H.D. and Miyojim, M. (1998). Automatic Pavement Distress Detection, *Journal of Information Science*, 108, pp. 219-240.
4. Tsai, Y.C., Kaul, V., and Mersereau, R.M. (2010). Critical Assessment of Pavement Distress Segmentation Methods, *Journal of Transportation Engineering*, 136(1), pp. 11-19.
5. Cuhadar, A., Shalaby, A., and Tasdoken S. (2002). Automatic Segmentation of Pavement Condition Data Using Wavelet Transform, *Proceedings of the Canadian Conference on Electrical and Computer Engineering*, Winnipeg, MB, Canada, pp.1009-1014.
6. Zhou, J., Huang, P.S., and Chiang, F.P. (2003). Wavelet Aided Pavement Distress Image Processing. *Proceedings of International Society for Optical Engineering (SPIE)*, 5207, pp. 728-739.
7. Zhou, J., Huang, P.S., and Chiang, F.P. (2006). Wavelet based Pavement Distress Detection and Evaluation, *Optical Engineering*, 45(2), pp. 1-10.

8. Javidi, B., Stephens, J., Kishk, S., Naughton, T., McDonald, J.J., and Issac, A. (2003). Pilot for Automated Detection and Classification of Road Surface Degradation Features, *Project Report No. JHR 03-293*, Connecticut Transportation Institute, Storrs, CT, USA, pp. 1-40.
9. Kingsbury, N. (1999). Image Processing with Complex Wavelets, *Philosophical Transactions of the Royal Society A: Mathematical, Physical & Engineering Sciences*, 357(1760), pp. 2543-2560.
10. Nejad, F.M. and Zakeri H. (2011). A Comparison of Multi-resolution Methods for Detection and Isolation of Pavement Distress, *Expert Systems with Applications*, 38, pp. 2857-2872.
11. Ying, L. and Salari, E. (2010). Beamlet Transform-based Technique for Pavement Crack Detection and Classification, *Computer-Aided Civil and Infrastructure Engineering*, 25, pp. 572-580.
12. Wang, K.C.P., Li, Q., and Gong, W. (2007). Wavelet-based Pavement Distress Image Edge Detection with a Troun Algorithm, *Transportation Research Record*, No. 2024, pp. 73-91.
13. Celik, T. and Tjahjadi, T. (2010). Unsupervised Colour Image Segmentation Using Dual-tree Complex Wavelet Transform, *Computer Vision and Image Understanding*, 114, pp. 813-826.
14. Chang, S.G., Yu, B., and Vetterli, M. (2000). Adaptive Wavelet Thresholding for Image Denoising and Compression, *IEEE Transactions on Image Processing*, 9(9), pp. 1532-1546.
15. Donoho, D.L. and Johnstone, M. (1994). Ideal Spatial Adaptation via Wavelet Shrinkage, *Biometrika*, 81, pp. 425-455.
16. Grgic, S., Grgic, M., and Zovko-Cihlar, B. (2001). Performance Analysis of Image Compression using Wavelets, *IEEE Transactions on Industrial Electronics*, 48(3), pp. 682-695.